Grain Rotation in Ion-Complexed Symmetric Diblock Copolymer Thin Films under an Electric Field

Jia-Yu Wang, Julie M. Leiston-Belanger, James D. Sievert, and Thomas P. Russell*

Department of Polymer Science and Engineering, University of Massachusetts, Amherst, Massachusetts 01003

Received June 26, 2006; Revised Manuscript Received August 23, 2006

ABSTRACT: In symmetric polystyrene-*block*-poly(methyl methacrylate) (PS-*b*-PMMA) diblock copolymer thin films, lithium−PMMA complexes were formed with the addition of lithium chloride (LiCl), significantly increasing both χ and dielectric constant. These led to a transition in the kinetic pathway of the orientation of lamellar microdomains under an applied electric field from a disruption and re-formation of the microdomains to a grain rotation mediated by movement of defects. By controlling the number of lithium−PMMA complexes, the microdomain alignment is possibly regulated in PS-*b*-PMMA copolymer thin films.

Diblock copolymers (BCPs) can self-assemble into periodic arrays of nanoscopic domains that have potential use in applications ranging from optics to microelectronics.[1−5] The microphase separation is driven by the nonfavorable interactions between the blocks. The degree of microphase separation is determined by χN, where χ is the Flory−Huggins segmental interaction parameter and N is the degree of polymerization. As shown experimentally[6−11] and theoretically,[12−19] an electric field can be effective means of aligning the microdomains in a desired direction. In this case, the applied field acts on the dielectric constant difference between the domains and the matrix. However, complete alignment of the microdomains in films is not always achieved due to the preferential interactions of one of the blocks with the electrodes confining the film.[11] Although Tsori and co-workers recently discussed an argument of "free-ion mechanism" which enhanced the ability of electric field to align diblock copolymer microdomains,[20,21] our experimental results have demonstrated that the formation of ion complexes in a symmetric polystyrene-*block*-poly(methyl methacrylate) (PS-*b*-PMMA) diblock copolymer played a significant role in the process of microdomain reorientation, even leading to a complete alignment of lamellar microdomains, as a consequence of an increased difference in the dielectric constants of the PS and PMMA microdomains.[22]

While the end result of the complexation is evident, the underlying mechanism of the rearrangement of the domains with the lithium−PMMA complexes is still unclear. For symmetric BCPs, several kinetic pathways of aligning lamellar microdomains have been proposed on the basis of computational simulations and experiments. Amundsen et al.[7,12] proposed two mechanisms: a selective electric-field-induced disordering and alignment through movements of defects. Only the latter mechanism was supported by the experimental results where the movement of edge dislocations was observed. De Rouchey et al.[23] and Xu et al.,[10] on the other hand, found that the reorientation of lamellar microdomains proceeded by a disruption or disordering of the original lamellar morphology, followed by a rotation of smaller grains in the direction of the applied field using in-situ small-angle X-ray scattering (SAXS) and transmission electron microscopy (TEM). Recently, Böker et al.[8,24] suggested that both defect translation and grain rotation occurred in studies of BCP solutions. In addition, simulations by Tsori et al. and Zvelindovsky et al. supported both mechanisms.[13,25,26] Nucleation and growth of microdomains by small-scale undulations typically occurred close to the order−disorder transition (ODT), while grain rotation happens in the more strongly phase-separated systems.[26,27] Here, we show that the formation of lithium−PMMA complexes in symmetric PS-*b*-PMMA diblock copolymer thin films induces a transition in the mechanism of the orientation of lamellar microdomains from a disruption and re-formation of the microdomains to a grain rotation mediated by movement of defects.

A PS-*b*-PMMA diblock copolymer with a number-average molecular weight (M_n) of 57 kg/mol, a polydispersity (PDI) of 1.09, and a PS volume fraction (f_{PS}) of 0.60 was used to study the mechanism of reorientating the BCP microdomains in a dc electric field of ~40 V/μm. The preparation of the BCP thin films, addition of lithium chloride (LiCl) into PS-*b*-PMMA, and the alignment experiment have been discussed previously.[22] The change in the morphology during alignment was measured by TEM and grazing incidence small-angle X-ray scattering (GISAXS). TEM experiments were performed on a JEOL TEM200CX at an accelerating voltage of 200 kV. GISAXS measurements were performed on the X22B beamline (National Synchrotron Light Source, Brookhaven National Laboratory) using X-rays having a wavelength of $\lambda = 1.517$ Å with an exposure time of 30 s per frame. Measurements were also performed on the 8-ID beamline (Advanced Photon Source, Argonne National Laboratory) using X-rays having a wavelength of $\lambda = 1.675$ Å with the exposure time of 10 s per frame. Typical GISAXS patterns are taken at an incidence angle of 0.2°, which is higher than the critical angle of the copolymer but lower than the critical angle of silicon substrate. Consequently, the beam penetrated through the entire BCP thin film.

PS-*b*-PMMA with a number-average molecular weight (M_n) of 62 kg/mol and dPS-*b*-PMMA (where d indicates perdeuteration of the PS block) with number-average molecular weight (M_n) of 56 and 115 kg/mol, a polydispersity (PDI) of 1.06, and a PS volume fraction (f_{PS}) of 0.53 were used to study the domain spacing D using small-angle X-ray scattering. dPS-*b*-PMMA with a number-average molecular weight (M_n) of 28 kg/mol, a polydispersity (PDI) of 1.06, and a PS volume fraction (f_{PS}) of 0.53 was used to study the characteristic segmental length by

* To whom correspondence should be addressed. E-mail: russell@mail.pse.umass.edu.

10.1021/ma0614287 CCC: $33.50
Published on Web 11/04/2006

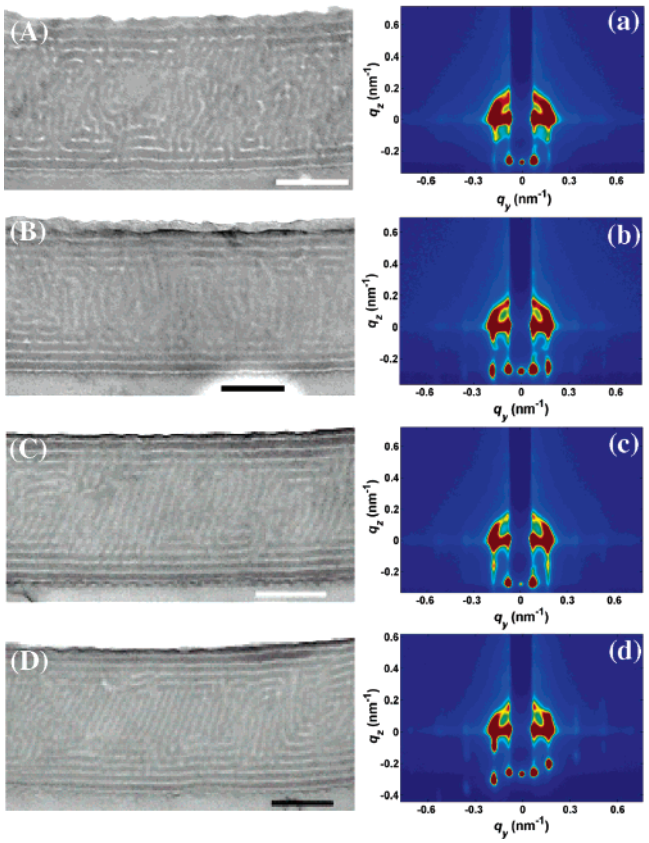

Figure 1. Left: cross-sectional TEM images of PS-*b*-PMMA thin films after applying a ~40 V/μm dc electric field at 175 ± 5 °C under N_2 for (A) 4, (B) 10, (C) 14, and (D) 20 h. Scale bar: 200 nm. Right: corresponding GISAXS pattern measured at $\alpha = 0.20°$.

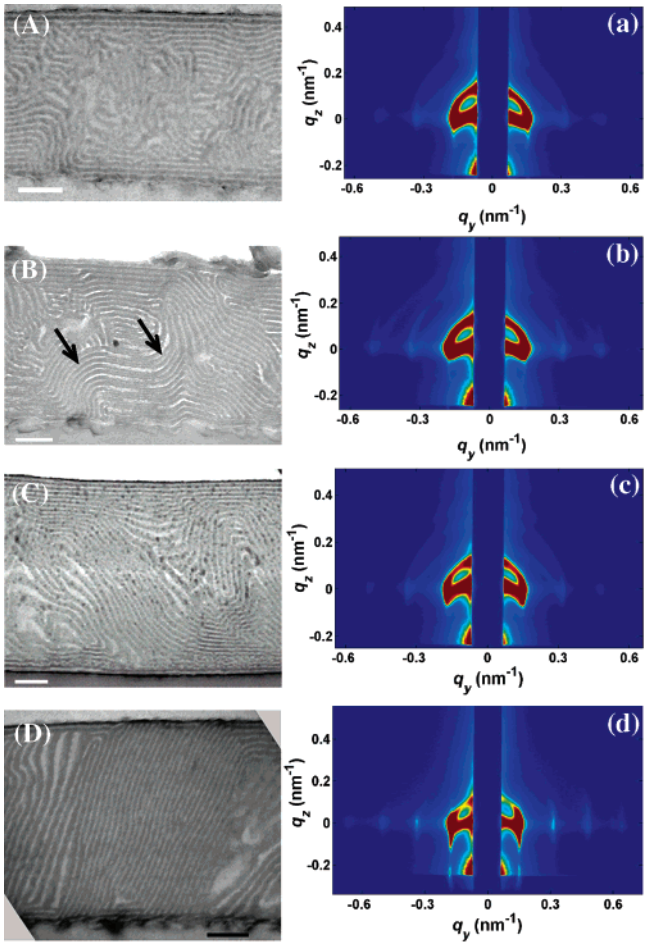

Figure 2. Left: cross-sectional TEM images of PS-*b*-PMMA thin films with lithium complexes after applying a ~40 V/μm dc electric field at 175 ± 5 °C under N_2 for (A) 4, (B) 10, (C) 14, and (D) 20 h. Scale bar: 200 nm. Right: corresponding GISAXS pattern measured at $\alpha = 0.20°$.

SAXS. The measurements are employed at room temperature under vacuum with the exposure time of 30 min, using an Osmic MaxFlux X-ray source with a wavelength λ of 1.54 Å. All SAXS samples with a thickness about ~0.5 mm are drop-cast on Kapton films, annealed at 170 °C under vacuum for 2 days, and then quenched to room temperature.

Figure 1 shows the alignment of lamellar microdomains in pure PS-*b*-PMMA thin films annealed at 175 ± 5 °C under a dc electric field of ~40 V/μm. The cross-sectional TEM images show that most lamellae are broken up into small pieces that are randomly oriented in the center of BCP films. However, several lamellar layers adjacent to the interfaces remain orientated parallel to the interface due to the preferential interactions of PMMA with the electrode interfaces (Figure 1A). The corresponding GISAXS patterns (Figure 1a), comprised of a ring of scattering, suggest that there is a random orientation of the microdomains in the center of the film. By increasing the annealing time under the applied field (Figure 1B), some of these small sections of the microdomains tend to align locally and recombine to form lamellae oriented parallel to the applied electric field direction. However, on average they are still randomly oriented in the film. The TEM results are mirrored by the GISAXS patterns where a diffuse ring is observed with some intensification along the q_y direction (Figure 1b). In a later intermediate stage, more recombinations of the lamellae occur to form lamellae oriented in the applied field direction (Figure 1C) and a further intensification of the scattering along the q_y direction (Figure 1c). This process continues with longer times as evidenced by the results in Figures 1d and 1D. Throughout the alignment the lamellar adjacent to the substrate remain oriented parallel to the interface, unaffected by the applied field. This is consistent with previous observations[10] and simulations,[28] where the dominant kinetic pathway of reorientating the lamellar microdomains in the pure BCP thin films is by a local disruption and re-formation of lamellae.

In contrast to the pure PS-*b*-PMMA, Figure 2 shows results for a thin film of PS-*b*-PMMA complexed with LiCl under the same experimental conditions. Despite the defects, the lamellar microdomains remain intact, forming randomly oriented grains initially (Figure 2A). Although there are lamellar microdomains adjacent to the interfaces, they do not completely cover the interfaces. With increasing the annealing time (Figure 2B), the defects propagate and annihilate when two of them meet, resulting in grains that increase in size with grain boundaries bent (indicated in arrows) in the direction of electric field. As the process continues (Figure 2C), the grains continue to grow until a critical size is reached, where upon they rotate into the direction of the applied electric field. Amundson et al. predicted the whole grains, whose sizes exceed a certain critical size of 150 nm, could be effectively rotated by an electric field.[29] This early prediction is in keeping with the results in Figure 2D, where larger grains are rotated into the field direction and extend from one surface of the film to the other. Large grains not only rotate by themselves, but they cause the orientation of adjacent smaller grains. This enhances the ability of the applied field to overcome preferential interfacial interactions and to eliminate defects, so that complete alignment of lamellar microdomains can be achieved. GISAXS results also provide evidence of a grain rotation mechanism. In the early and intermediate stages

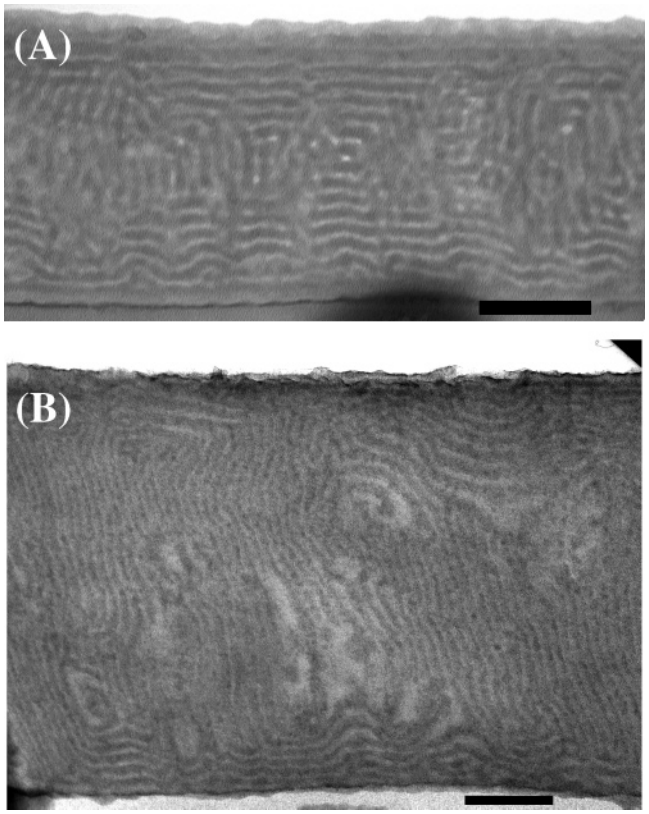

Figure 3. Cross-sectional TEM images of PS-*b*-PMMA thin films with molar ratios of added LiCl to the carbonyl group in PMMA: (A) 1:10, (B) 1:6 after applying a ~40 V/μm dc electric field at 175 ± 5 °C under N_2 for 20 h. Scale bar: 200 nm.

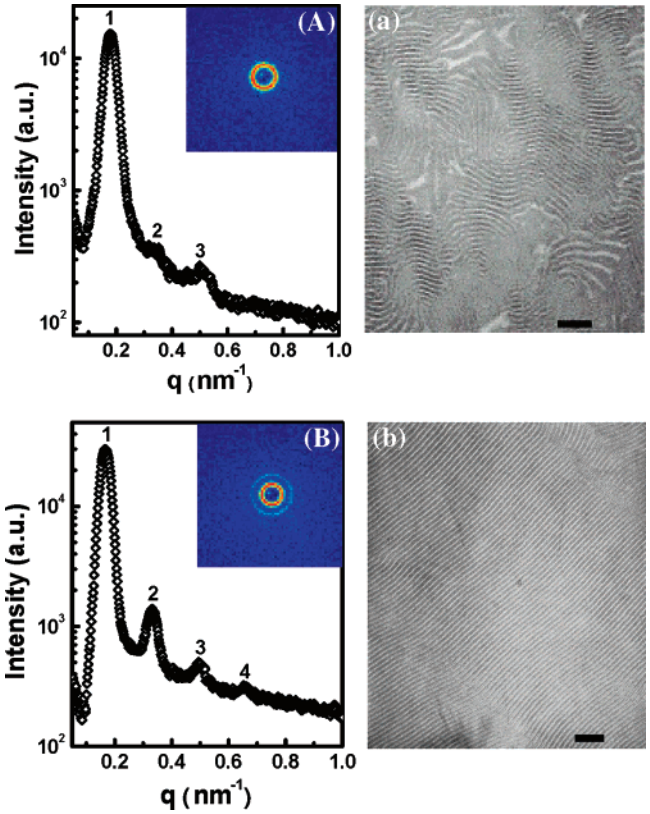

Figure 4. Left: SAXS profiles of (A) PS-*b*-PMMA and (B) PS-*b*-PMMA with lithium complexes after annealing at 170 °C for 2 days (no electric field was applied) followed by quenching to room temperature. Inset: corresponding 2-D SAXS images. Right: corresponding TEM images. Scale bar: 200 nm.

(Figure 2a,b), the GISAXS patterns exhibit an isotropic scattering ring due to the random orientation of the grains. The relative scattering intensities increase as the annealing time increases, since the growth of grains promotes further microphase separation. After annealing 14 h (Figure 2c), the isotropic scattering ring changes into arcs, indicating that grains are effectively rotated by the electric field. In the q_z direction, the scattering remains very strong, arising from grains oriented parallel to the interfaces, whereas the scattering of pure PS-*b*-PMMA copolymers (Figure 1c) is relatively weak since only several parallel lamellae exist near the interfaces. Near the final stages of orientation (Figure 2d), the scattering rods are seen along the q_y direction, and the scattering in the q_z direction significantly decreases, suggesting that most of BCP grains are rotated normal to the surface. Furthermore, such a mechanism transition can also be observed from the cross-sectional TEM images of PS-*b*-PMMA thin films with an increasing molar ratio of added LiCl to the carbonyl group in PMMA (Figure 3). In the diblock copolymer thin films with a molar ratio of added LiCl to the carbonyl group in PMMA of 1:10 (Figure 3a), there still exist some small pieces of broken lamellar microdomains even after applying the electric field for 20 h, similar to the situation in the pure diblock copolymer thin films, indicating that fluctuations are still predominant and do not allow gains grow large enough to rotate due to an insufficient concentration of lithium−PMMA complexes. As the molar ratio of added LiCl to the carbonyl group in PMMA is increased to 1:6, a similar kinetic pathway to reorient the lamellar microdomains was observed (images were not shown) as the sample with the molar ratio of added LiCl to the carbonyl group in PMMA of 1:1 (Figure 2); i.e., the grains become larger and larger and eventually rotate to the direction of electric field (Figure 3b). Thus, both TEM and GISAXS results indicate that in the presence of sufficient lithium−PMMA complexes grain rotation mediated by defect movement is the dominant mechanism of reorientating the microdomains in thin films of PS-*b*-PMMA under a dc electric field.

Usually, grain rotation is not possible in the BCP thin films due to the geometric constraint of the film thickness[10] and occurs in strong segregation regime.[8,26,27,30] For pure PS-*b*-PMMA copolymer used in our studies, χN is about 22. [31] Consequently, the copolymer is in the intermediate separation, that is, neither the strong nor weak segregation regime. Yet, with the lithium−PMMA complexes, a transition in the orientation mechanism to grain rotation is evident. Furthermore, the q_y scan of the GISAXS pattern at $q_z = 0$ nm^{-1} (not shown here) shows that, in thin films, the equilibrium domain spacing D ($D = 2\pi/q^*$) for PS-*b*-PMMA complexed with lithium is 38.5 nm, more than 2 nm greater than the period of the pure PS-*b*-PMMA. SAXS results of bulk copolymers show a similar increase of the equilibrium domain spacing D for PS-*b*-PMMA complexed with lithium from 35.5 for pure PS-*b*-PMMA to 37.7 nm for the complexed PS-*b*-PMMA (Figure 4). This increasing D after the formation of complexes in copolymers is consistent with recently published results.[32−35] The corresponding TEM images show that numerous defects exist in a ~2 × 2 μm^2 area of for pure PS-*b*-PMMA, whereas the grain sizes of PS-*b*-PMMA copolymers with the lithium complexes are so much larger that grain boundaries cannot be seen over similar areas (Figure 4). These results suggest that χ must be significantly increased with the formation of lithium−PMMA complexes.[33,34]

As is well-known, the equilibrium domain spacing D satisfies the relationship $D \sim aN^{2/3}\chi^{1/6}$ in the strong segregation limit (SSL).[1] To quantify the increased χ, SAXS measurements were performed on PS-*b*-PMMA (M_n = 62 kg/mol) and dPS-*b*-

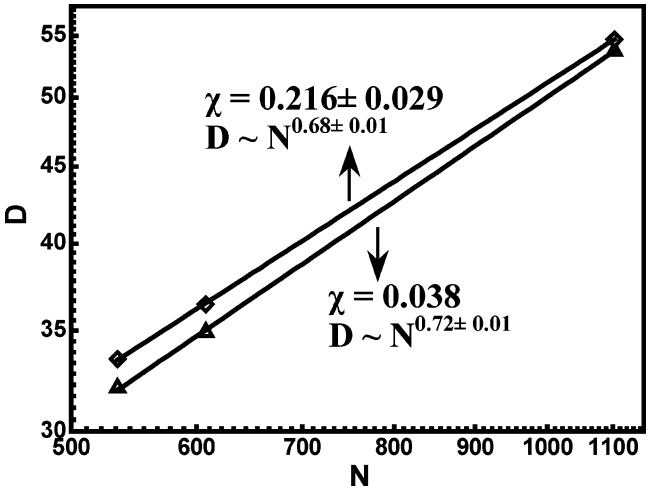

Figure 5. Domain spacing, *D*, vs chain length, *N*, in a double-logarithmic plot. Triangle: data from PS-*b*-PMMA copolymers; diamond: data from corresponding PS-*b*-PMMA copolymers with lithium complexes. Full lines: nonlinear least-squares fitting with an R^2 of 0.999 for each line in the range $N = 535-1102$.

PMMA ($M_n = 56$ and 115 kg/mol) with and without lithium complexes. In the scattering patterns from ordered, lamellar samples, Bragg reflections are observed at scattering vectors $q = q_k = kq^*$, where k is an odd integer, $q = 4\pi/\lambda \sin(\theta/2)$ is the scattering vector, λ is the wavelength, and θ is the scattering angle. The third-order reflections q_3 are used to determine domain spacing D because of the smaller relative error.[36] In the strong segregation regime, where the interfacial thickness is sufficiently small compared to D, the 2/3 power law is satisfied, i.e., $D \sim N^{2/3}$.[36,37] Figure 5 shows domain spacing D vs chain length N on a double-logarithmic scale for these three copolymers ($N = 535$, 608, and 1102) without ionic complexes or with equally concentrated lithium−PMMA complexes. To establish the scaling relationship, $D \sim N^a$, nonlinear least-squares fits to the data gave $a = 0.72$ for pure copolymers and 0.68 for the copolymers complexed with lithium. The high exponent for pure copolymers arises from the fact that they are located in an intermediate segregation regime between weak and strong segregation state, and the assumption of narrow interface is not valued.[36,38] The 2/3 exponent for the complexed copolymers indicates that the complexation has moved the copolymer into the strong segregation regime. The fitting of SAXS of the copolymer in the disordered state using arguments of Leibler[1,40] indicates that there is no significant change in the radius of gyration (R_g) of PS-*b*-PMMA copolymers ($M_n = 28$ kg/mol) before and after the formation of lithium−PMMA complexes. This suggests that the formation of lithium−PMMA complexes has little influence on the characteristic segmental length, a, of the PMMA. If we use this for PS-*b*-PMMA in the strong segregation regime, then χ for PS-*b*-PMMA copolymers with lithium−PMMA complexes is calculated to be 0.210, since $D \sim aN^{2/3}\chi^{1/6}$ ($\chi = 0.038$ for pure PS-*b*-PMMA copolymers[31]). Therefore, the electric field experiments for the complexed PS-*b*-PMMA copolymers are done in the strong segregation regime, so that grain rotation can occur.

Recently, computational simulation by Lyaknova et al. also suggested that grain rotation may be a dominant mechanism of realignment in BCP thin films in the strong separation regime, but a highly defected structure remained even at the final stage due to the geometric confinement.[40] In our system, defects are almost completely removed due to the increased χ and dielectric contrast between two blocks. Both χ and the dielectric contrast are further increased as the number or concentration of lithium−PMMA complexes increases. After annealing under an applied field for 24 h complete alignment of the microdomains is achieved (Figure 6).

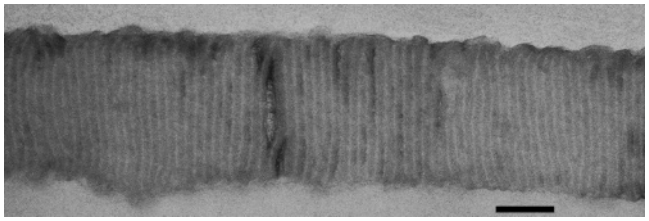

Figure 6. Cross-sectional TEM image of PS-*b*-PMMA thin film with almost saturated lithium−PMMA complexes after annealing at 175 ± 5 °C in N_2 environment under a dc electric field of ~40 V/mm for 24 h.

In conclusion, we have found that, in thin films, under an applied electric field, the formation of lithium complexes with PMMA in PS-*b*-PMMA enables a grain rotation mediated by the movement of defects to bring about an alignment of lamellar microdomains. The mechanism, normally found in copolymers in the strong segregation limit, is enabled by the increase in χ and dielectric constant with the complex formation in thin films. Concentration fluctuations at the interface between the microdomains are suppressed due to the increase in the interface tension. By controlling the number of lithium−PMMA complexes, the microdomain alignment is possibly regulated in PS-*b*-PMMA copolymer thin films.

Acknowledgment. We thank B. Ocko, X. Li, J. Wang, K. Cavicchi, M. Misner, J. He, and R. Tangirala for assistance with the GISAXS experiments. This work was supported by the Department of Energy Basic Energy Science (DEFG0296ER45612) and the National Science Foundation-supported Material Research Science and Engineering Center at the University of Massachusetts, Amherst (DMR-0213695).

References and Notes

(1) Hamley, I. W. In *The Physics of Block Copolymers*; Oxford University Press: New York, 1998.
(2) Hadjichristidis, N.; Pispas, S.; Floudas, G. In *Block Copolymers: Synthetic Strategies, Physical Properties, and Applications*; John Wiley & Sons: New York, 2002.
(3) Bates, F. S.; Fredrickson, G. H. *Phys. Today* **1999**, *52*, 32.
(4) Lodge, T. P. *Macromol. Chem. Phys.* **2003**, *204*, 265.
(5) Hawker, C. J.; Russell, T. P. *MRS Bull.* **2005**, *30*, 952.
(6) Morkved, T. L.; Lu, M.; Urbas, A. M.; Ehrichs, E. E.; Jaeger, H. M.; Mansky, P.; Russell, T. P. *Science* **1996**, *273*, 931.
(7) Amundson, K.; Helfand, E.; Quan, X.; Smith, S. D. *Macromolecules* **1993**, *26*, 2698.
(8) Böker, A.; Elbs, H.; Hänsel, H.; Knoll, A.; Ludwigs, S.; Zettl, H.; Urban, V.; Abetz, V.; Müller, A. H. E.; Krausch, G. *Phys. Rev. Lett.* **2002**, *89*, 135502.
(9) Thurn-Albrecht, T.; DeRouchey, J.; Russell, T. P.; Kolb, R. *Macromolecules* **2002**, *35*, 8106.
(10) Xu, T.; Zhu, Y.; Gido, S. P.; Russell, T. P. *Macromolecules* **2004**, *37*, 2625.
(11) Xu, T.; Hawker, C. J.; Russell, T. P. *Macromolecules* **2003**, *36*, 6178.
(12) Amundson, K.; Helfand, E.; Quan, X.; Hudson, S. D.; Smith, S. D. *Macromolecules* **1994**, *27*, 6559.
(13) Tsori, Y.; Andelman, D. *Macromolecules* **2002**, *35*, 5161.
(14) Thurn-Albrecht, T.; DeRouchey, J.; Russell, T. P.; Jaeger, H. M. *Macromolecules* **2000**, *33*, 3250.
(15) Pereira, G. G.; Williams, D. R. M. *Macromolecules* **1999**, *32*, 8115.
(16) Ashok, B.; Muthukumar, M.; Russell, T. P. *J. Chem. Phys.* **2001**, *115*, 1559.
(17) Matsen, M. W. *Phys. Rev. Lett.* **2005**, *95*, 258302.
(18) Tsori, Y.; Andelman, D.; Lin, C.; Schick, M. *Macromolecules* **2006**, *39*, 289.
(19) Lin, C. Y.; Schick, M. Submitted for publication.
(20) Tsori, Y.; Tournilhac, F.; Andelman, D.; Leiber, L. *Phys. Rev. Lett.* **2003**, *90*, 145504.
(21) Tsori, Y.; Tournilhac, F.; Leibler, L. *Macromolecules* **2003**, *36*, 5873.

(22) Wang, J. Y.; Xu, T.; Leiston-Belanger, J.; Gupta, S.; Russell, T. P. *Phys. Rev. Lett.* **2006**, *96*, 128301.
(23) DeRouchey, J.; Thurn-Albrecht, T.; Russell, T. P.; Kolb, R. *Macromolecules* **2004**, *37*, 2538.
(24) Böker, A.; Knoll, A.; Elbs, H.; Abetz, V.; Müller, A. H. E.; Krausch, G. *Macromolecules* **2002**, *35*, 1319.
(25) Kyrylyuk, A. V.; Zelindovsky, A. V.; Sevink, G. J. A.; Fraaije, J. G. E. M. *Macromolecules* **2002**, *35*, 1473.
(26) Zvelindovsky, A. V.; Sevink, G. J. A. *Phys. Rev. Lett.* **2003**, *90*, 049601.
(27) Schmidt, K.; Böker, A.; Zettl, H.; Schubert, F.; Hänsel, H.; Fischer, F.; Weiss, T. M.; Abetz, V.; Zvelindovsky, A. V.; Sevink, G. J. A.; Krausch, G. *Langmuir* **2005**, *21*, 11974.
(28) Kyrylyuk, A. V.; Sevink, G. J. A.; Zvelindovsky, A. V.; Fraaije, J. G. E. M. *Macromol. Theory Simul.* **2003**, *12*, 508.
(29) Amundson, K.; Helfand, E.; Davis, D. D.; Quan, X.; Patel, S. S.; Smith, S. D. *Macromolecules* **1991**, *24*, 6546.
(30) Böker, A.; Elbs, H.; Hänsel, H.; Knoll, A.; Ludwigs, S.; Zettl, H.; Zvelindovsky, A. V.; Sevink, G. J. A.; Urban, V.; Abetz, V.; Müller, A. H. E.; Krausch, G. *Macromolecules* **2003**, *36*, 8078.
(31) Russell, T. P.; Hjelm, R. P., Jr.; Seeger, P. A. *Macromolecules* **1990**, *23*, 890.
(32) Ruzette, A. G.; Soo, P. P.; Sadoway, D. R.; Mayes, A. M. *J. Electrochem. Soc.* **2001**, *148*, A537.
(33) Epps, III, T. H.; Bailey, T. S.; Pham, H. D.; Bates, F. S. *Chem. Mater.* **2002**, *14*, 1706.
(34) Epps, III, T. H.; Bailey, T. S.; Waletzko, R.; Bates, F. S. *Macromolecules* **2003**, *36*, 2873.
(35) Lee, D. H.; Kim, H. Y.; Kim, J. K.; Huh, J.; Ryu, D. Y. *Macromolecules* **2006**, *39*, 2027.
(36) Papadakis, C. M.; Almdal, K.; Mortensen, K.; Posselt, D. *J. Phys. II* **1997**, *7*, 1829.
(37) Ohta, T.; Kawasaki, K. *Macromolecules* **1986**, *19*, 2621.
(38) Papadakis, C. M.; Almdal, K.; Mortensen, K.; Posselt, D. *Europhys. Lett.* **1996**, *36*, 289.
(39) Leibler, L. *Macromolecules* **1980**, *13*, 1602.
(40) Lyakhova, K. S.; Zvelindovsky, A. V.; Sevink, G. J. A. *Macromolecules* **2006**, *39*, 3024.

MA0614287